Electronic Supplementary Material (ESI) for Nanoscale.

Supporting Information

A multiscale approach to assess thermomechanical performance and force generation in nanorobotic microgels

Chen Wang,[a,b,c] Philipp Harder,[a,b,c] Nergishan Iyisan,[a,b,c] Bolin Li,[a] Lukas Hiendlmeier,[c,d] Bernhard Wolfrum,[c,d] and Berna Özkale*[a,b,c]

[a] *Microrobotic Bioengineering Lab, School of Computation, Information, and Technology, Department of Electrical Engineering, Technical University of Munich, Hans-Piloty-Straße 1, Garching 85748, Germany. Email: berna.oezkale@tum.de*

[b] *Munich Institute of Robotics and Machine Intelligence, Technical University of Munich, Georg-Brauchle-Ring 60, 80992 Munich, Germany.*

[c] *Munich Institute of Biomedical Engineering, Technical University of Munich, Boltzmannstraße 11, 85748 Garching, Germany*

[d] *Neuroelectronics, School of Computation, Information, and Technology, Department of Electrical Engineering, Technical University of Munich, Hans-Piloty-Straße 1, Garching 85748, Germany.*

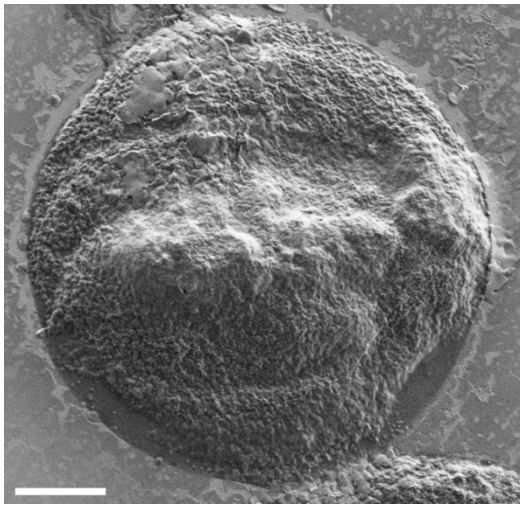

Fig. S1 Scanning electron microscopy image of a nanorobotic microgel with nanoactuators at 40 mg/ml. Scale bar: 10 µm.

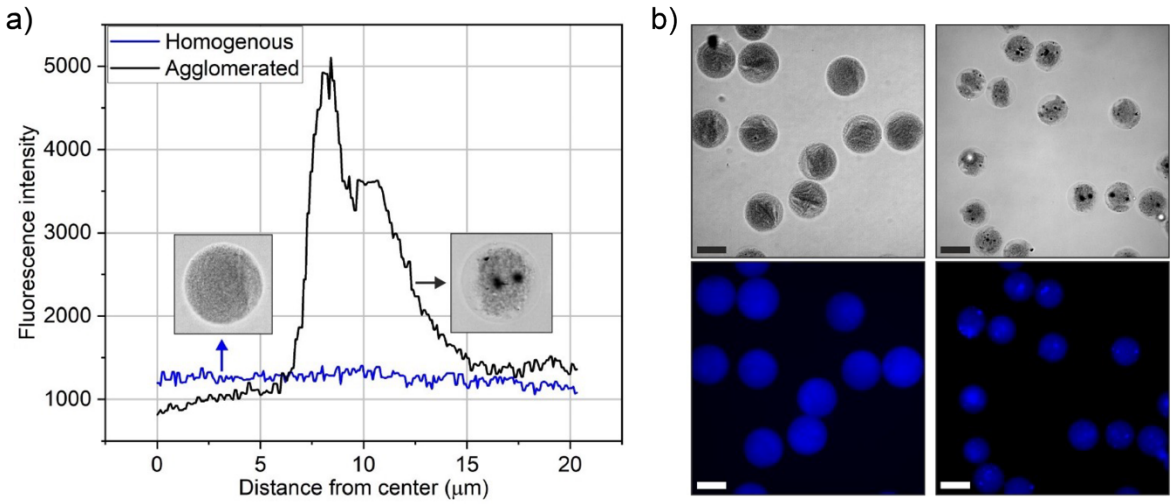

Fig. S2 (a) Fluorescence distribution over the radii of two microgels with either homogeneously distributed or heterogeneously distributed nanoactuators. (b) Brightfield and fluorescent images of homogeneous (left column) and heterogeneous (right column) microgels. Heterogeneity was due to the microfluidic device, leading to nanoactuator agglomerations and their non-uniform distribution as observed in the images on the right. Scale bar: 40 µm

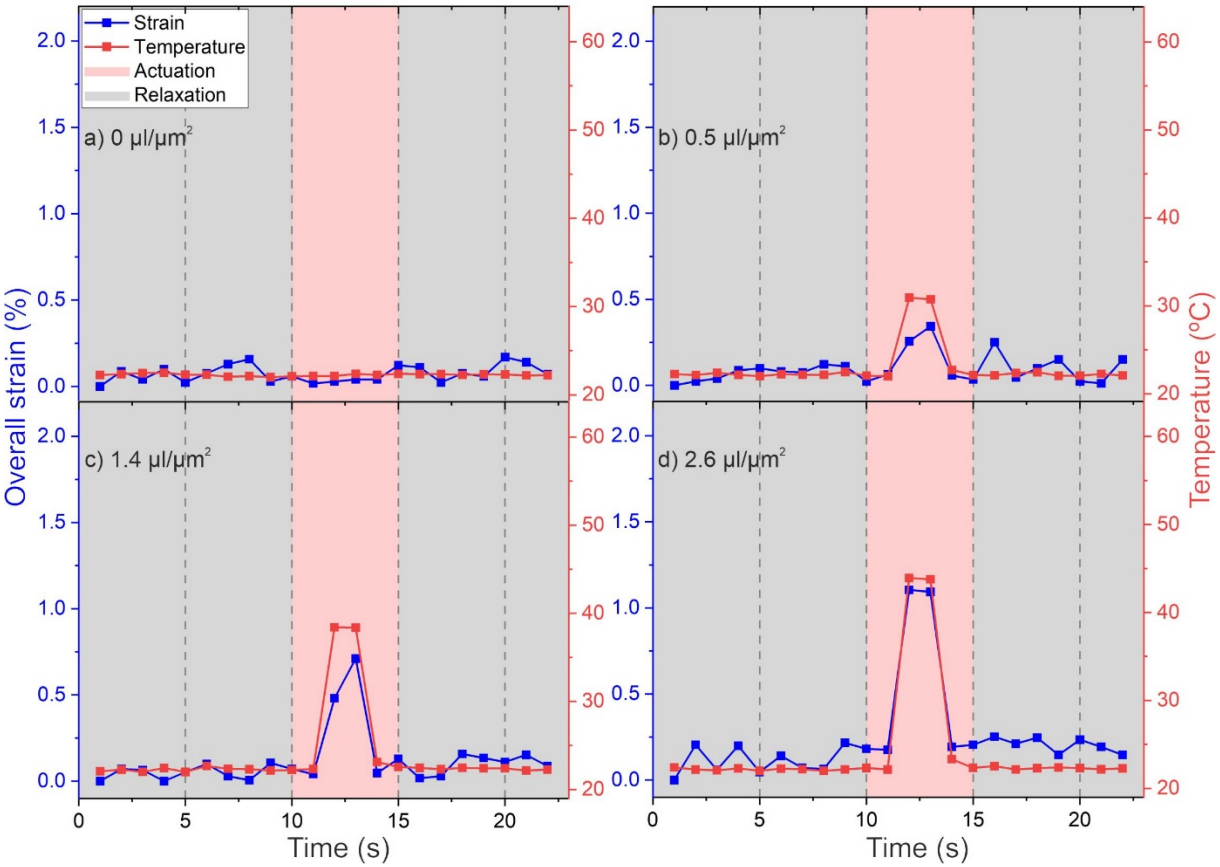

Fig. S3 (a) - (d) Thermomechanical characterization of a nanorobotic microgel actuated at varying laser intensities. The laser on time was fixed to 2 seconds to ensure strain saturation.

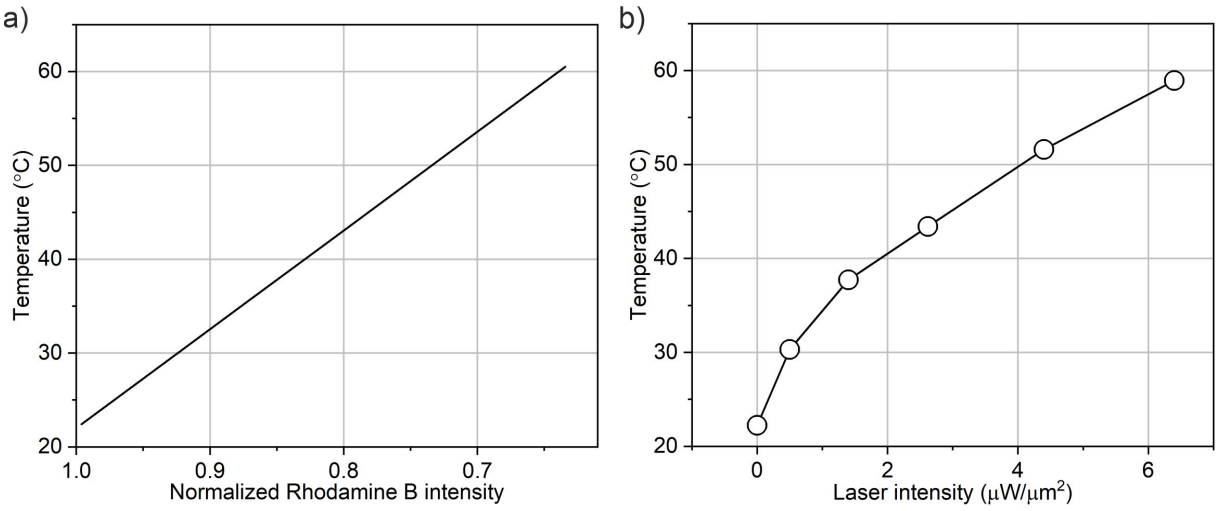

Fig. S4 (a) Temperature calibration based on the relationship of normalized Rhodamine B intensity and local temperature. (b) Correlation of laser intensity to microgel temperature, determined using the temperature calibration function.

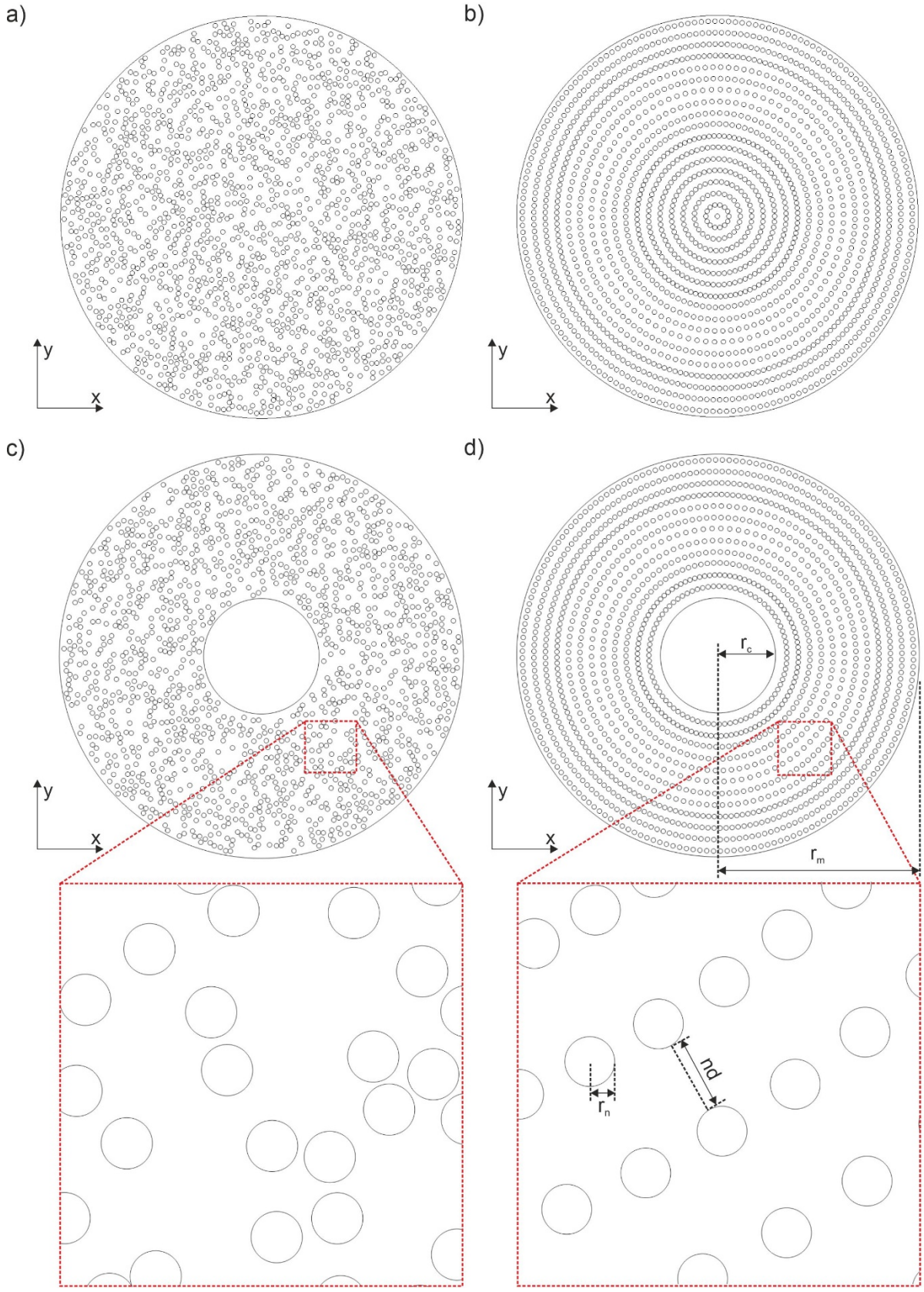

Fig. S5 Schematic representation of FE simulation setup. The ideal representative model is established with uniformly distributed nanoactuators arranged in a circular-packed pattern, and

the realistic microgel model is designed considering the spatial randomness of nanoactuators. 2D geometries of (a) realistic microgel model and (b) ideal representative model are employed in the case of cell-free microgels. 2D geometries of (c) realistic model and (d) ideal model are employed in the case of cell-laden microgels.

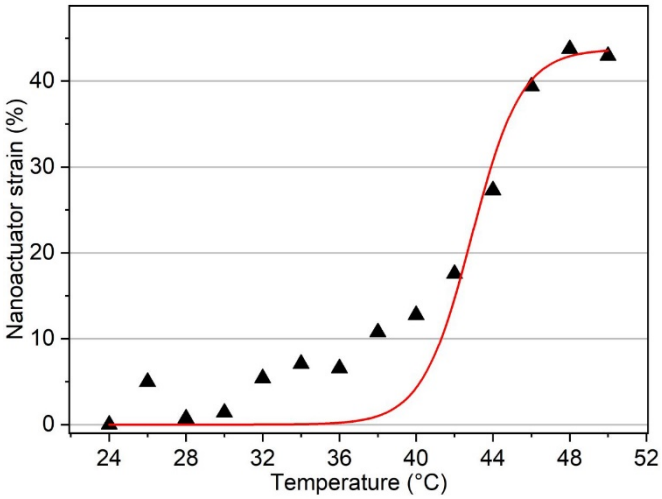

Fig. S6 Boltzmann fit for nanoactuator strain versus the corresponding local temperature.

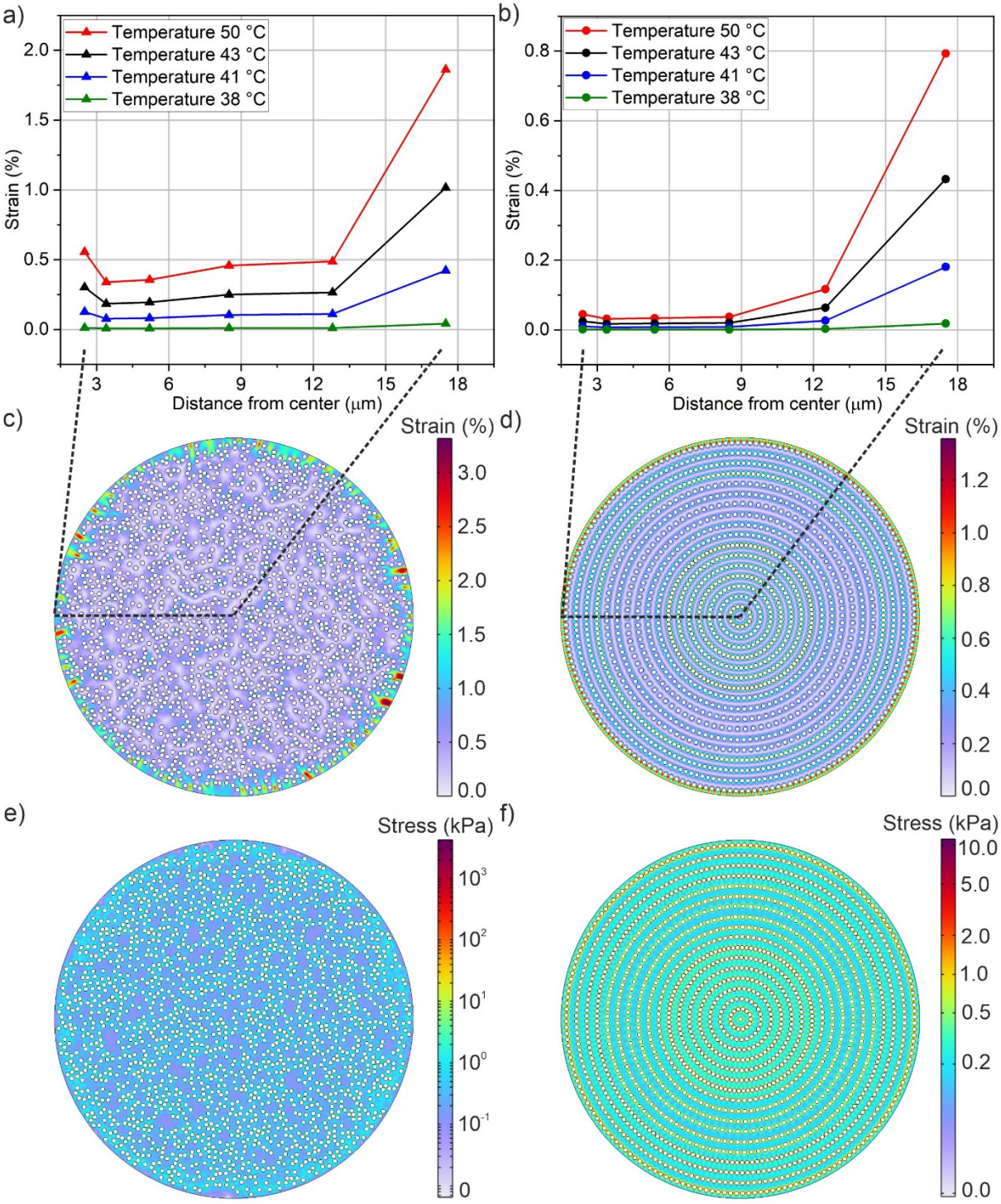

Fig. S7 Modeling of strain and stress in nanorobotic microgels through realistic and ideal models. (a) Microgel strain over radius is related to local temperature in the realistic spatial distribution of nanoactuators using RMM. Microgel radius: 17.5 μm. (b) Microgel strain over radius is correlated to local temperature in the ideal distribution of nanoactuators using IRM. (c) Microgel strain is mapped via RMM in a random nanoactuator distribution with a volume fraction of 26.4 vol% (40 mg/ml). (d) 2D mapping of microgel strain with 26.4 vol%

nanoactuators in an ideal circular-packed pattern with a mutual distance of 150 nm using IRM. (e) Microgel stress is mapped via RMMs in a random nanoactuator distribution with a volume fraction of 26.4 vol% (40 mg/ml). (f) 2D mapping of microgel stress with 26.4 vol% (40 mg/ml) nanoactuators in an ideal circular-packed pattern with a mutual distance of 150 nm using IRM.

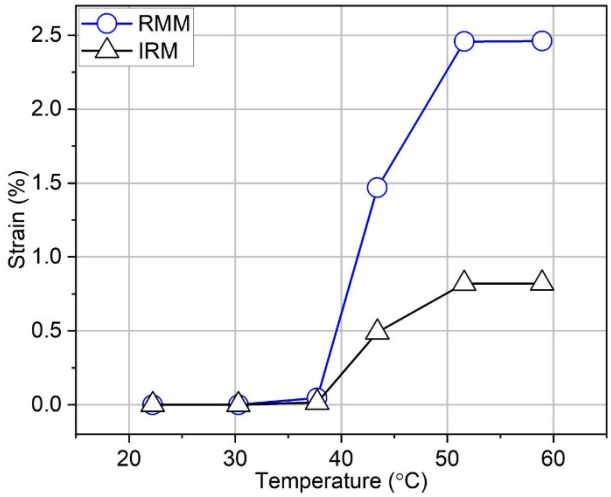

Fig. S8 Comparative analysis of microgel strain using the ideal representative (IRM) and realistic microgel models (RMM). Volume fraction of nanoactuators: 26.4 % (40 mg/ml). Microgel radii: 17.5 µm.

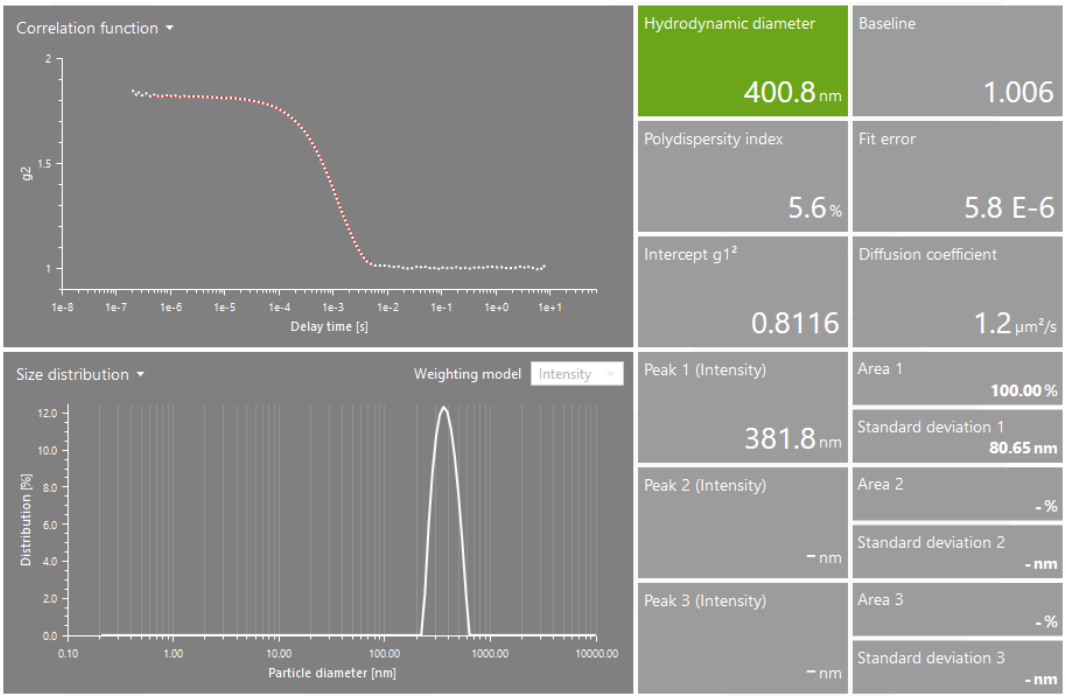

Fig. S9 A single intensity peak in a DLS analysis indicates the isotropic geometry of nanoactuators.

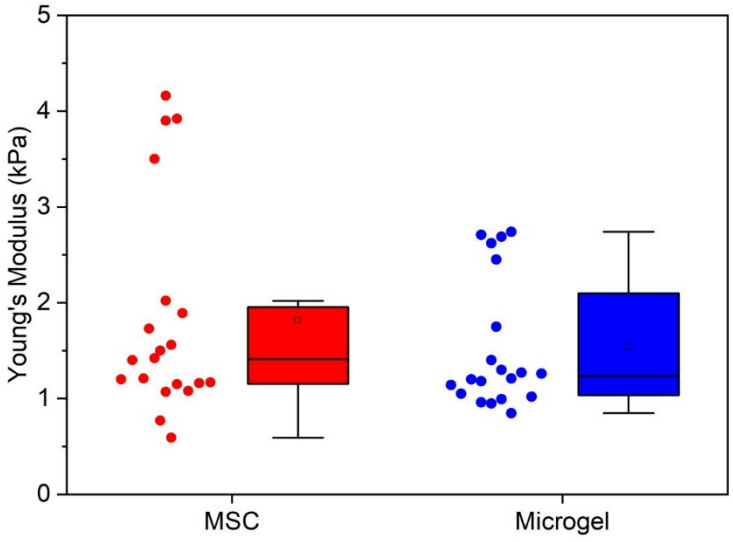

Fig. S10 Nanoindentation measurements showing the Young's modulus of mesenchymal stem cell (n = 20) and microgels (n = 20).

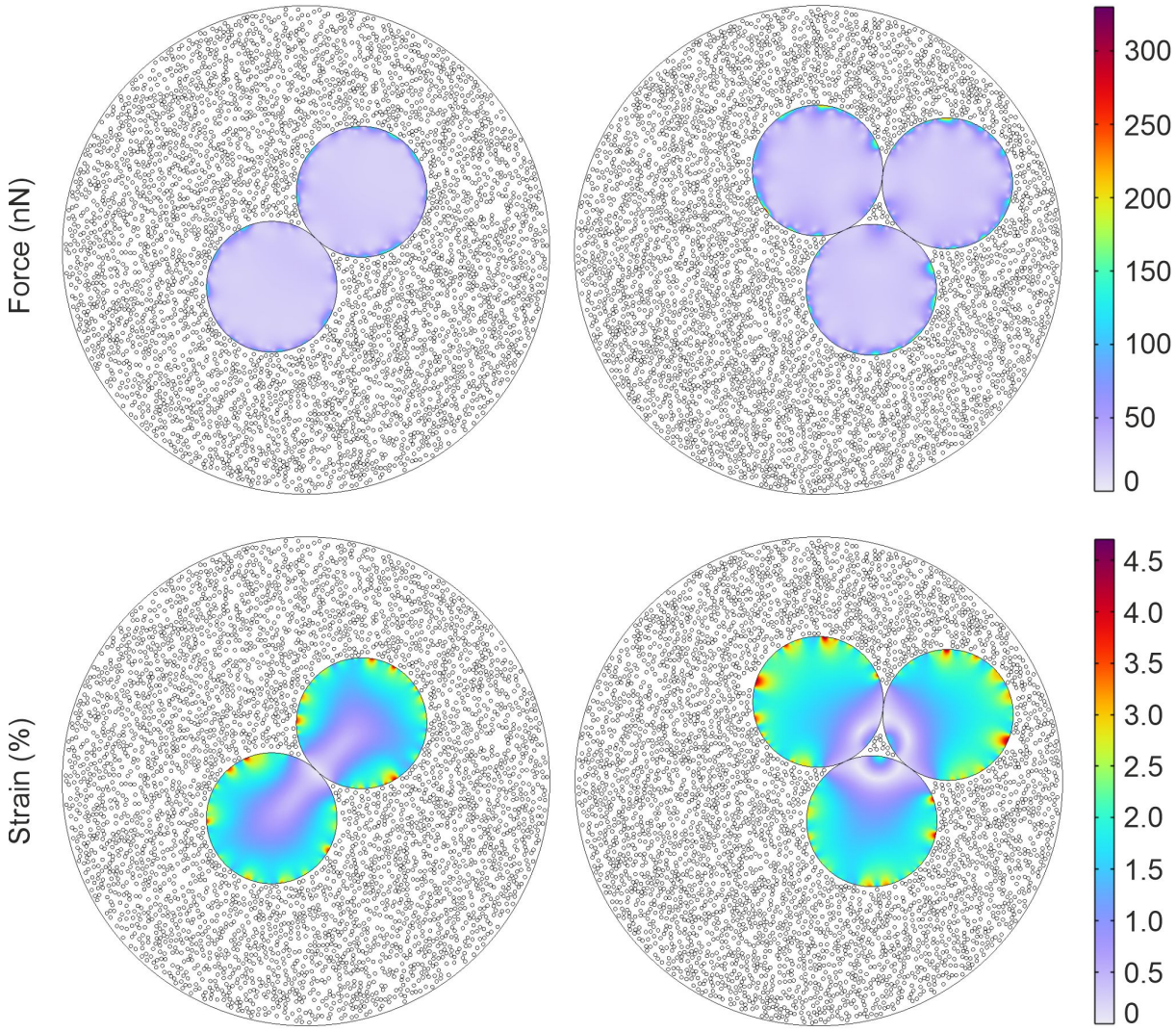

Fig. S11 Multicellular microgel simulation is performed to visualize force and strain distribution with 26.4 vol% (40 mg/ml) nanoactuators.